

# PROCEEDINGS OF SPIE

[SPIDigitalLibrary.org/conference-proceedings-of-spie](https://spiedigitallibrary.org/conference-proceedings-of-spie)

## Towards solid-state beam steering using a 7-emitter 1550 nm optical phased array

James T. Spollard, David R. Gozzard, Lyle E. Roberts, Paul G. Sibley, Samuel P. Francis, et al.

James T. Spollard, David R. Gozzard, Lyle E. Roberts, Paul G. Sibley, Samuel P. Francis, David E. McClelland, Daniel A. Shaddock, "Towards solid-state beam steering using a 7-emitter 1550 nm optical phased array," Proc. SPIE 10910, Free-Space Laser Communications XXXI, 109101P (4 March 2019); doi: 10.1117/12.2508951

**SPIE.**

Event: SPIE LASE, 2019, San Francisco, California, United States

# Towards solid-state beam steering using a 7-emitter 1550 nm optical phased array

James T. Spollard<sup>a,b,c</sup>, David R. Gozzard<sup>a,c</sup>, Lyle E. Roberts<sup>a,b,c</sup>, Paul G. Sibley<sup>a,b,c</sup>, Samuel P. Francis<sup>d</sup>, David E. McClelland<sup>a,b</sup>, and Daniel A. Shaddock<sup>a,b,c</sup>

<sup>a</sup>Research School of Physics and Engineering, The Australian National University, Canberra, ACT, Australia

<sup>b</sup>OzGrav-ANU, Centre for Gravitational Physics, The Australian National University, Canberra, ACT, Australia

<sup>c</sup>EQUUS-ANU, Centre for Gravitational Physics, The Australian National University, Canberra, ACT, Australia

<sup>d</sup>Jet Propulsion Laboratory, California Institute of Technology, Pasadena, California, US

## ABSTRACT

We present the preliminary design and experimental results of a 1550 nm solid-state beam pointing system based on an optical phased array (OPA) architecture. OPAs manipulate the distribution of optical power in the far-field by controlling the phase of individual emitters in an array. This allows OPAs to steer the beam in the far field without any mechanical components (e.g., steering mirrors). The beam-steering system presented here uses waveguide electro-optic modulators to actuate the phase of each element in a 7-emitter OPA, enabling kHz bandwidth steering with sub-milliradian pointing precision. The control system used to stabilize and control the phase of each emitter in the OPA exploits a technique called digitally enhanced heterodyne interferometry, allowing the phase of each emitter to be measured simultaneously at a single photodetector, dramatically simplifying the optical system. All digital signal processing is performed using a field-programmable gate-array. Applications of this technology include free-space link acquisition and tracking for satellite-to-satellite laser communications and light detection and ranging (LiDAR).

**Keywords:** coherent combination, optical phased array, FPGA

## 1. INTRODUCTION

Agile beam-steering technology is needed to service long range free space laser links in a growing number of use cases. Ground and space-based free space optical communication networks need beam steering for initial link acquisition and maintaining target lock when movement occurs. For example, the Laser Lunar Communication Demonstrator by MIT and NASA used a 2-axis gimbal system<sup>1</sup> to maintain the transmitting aperture pointing towards earth. The pair of satellites used in the GRACE-FO mission by NASA used a piezo-actuated fast steering mirror<sup>2</sup> for the link acquisition scan between the satellites at a distance of over 200km. Light Detection And Ranging (LiDAR) systems also requires high speed beam steering devices to rapidly and precisely interrogate a field of regard. They need to scan over a large area with typical scan rates of 10's of Hertz and be able to withstand harsh operating environments with little maintenance for many years at a time.<sup>3</sup>

Conventional beam steering technologies such as fast steering mirrors, Risley prisms and galvanometers rely on mechanical actuation, consequently their steering bandwidth is typically limited to a few kHz by inertia and other physical restrictions. These systems can also experience mechanical degradation over time with continual usage, making them a more risk-prone option for space-based or long-lifetime applications since it is difficult or expensive to repair them if they malfunction. Solid-state beam-steering technologies do not experience the same limitations as their mechanical counterparts and have the potential to become a robust alternative in a variety of applications that require agile beam-steering.

---

The primary author can be contacted at: james.spollard@anu.edu.au

Free-Space Laser Communications XXXI, edited by Hamid Hemmati,  
Don M. Boroson, Proc. of SPIE Vol. 10910, 109101P · © 2019 SPIE  
CCC code: 0277-786X/19/\$18 · doi: 10.1117/12.2508951

An Optical Phased Array (OPA) provides a way to coherently combine multiple spatially separated emitters into a contiguous and coherent wavefront in the far field. To achieve coherent beam combination, the relative phase of each emitter at the output needs to be stabilized. This typically involves measuring the phase of the individual emitters to monitor and compensate for any phase fluctuations introduced by relative path length variations due to uncommon fiber phase-noise resulting from thermal changes and acoustic vibrations. Since the location within the wavefront of the point of maximum intensity is dependent on the relative phases of each emitter, the position of the central lobe of maximum power can be maneuvered around the field of view by changing the relative phase of each of the output emitters. This redistributes optical power in the far field which has the effect of ‘steering’ the main central lobe of constructively interfered light. OPA’s also have the advantage of being able to create beams with significantly higher optical power than single emitter systems by combining multiple high-powered lasers into a single wavefront. This has advantages for long-range free space optical communication systems where power budgets are slim.

The aim of our demonstration system described in this proceeding is to demonstrate observable beam steering using an externally sensed OPA. Previous work at The Australian National University (ANU) by Roberts et al.<sup>4-6</sup> used a 3-emitter OPA to demonstrate high power handling, internally sensed architecture, and digital phasemeters. By changing the system architecture to a more simple externally sensed arrangement, which is easier to scale up, we implemented a 7-emitter OPA.

### 1.1 Optical Phased Arrays (OPA)

Optical phased arrays are capable of manipulating the distribution of optical power in the far field by coherently combining the light from multiple spatially separate transmit apertures. Maximum optical power in the far field occurs when light from each emitter in the array interferes constructively. Minimum power occurs when they interfere destructively. By controlling the location at which the emitters interfere constructively it is possible to ‘steer’ the outgoing beam without the need for mechanical beam-steering technologies (e.g., steering mirrors or Risley prisms). One way to do this is to precisely control the phase of the light exiting each emitter in the array.

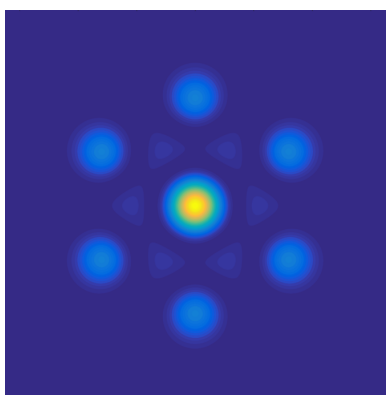


Figure 1. Simulation of far field wavefront with coherent combination of 7 emitters using a tiled aperture OPA.

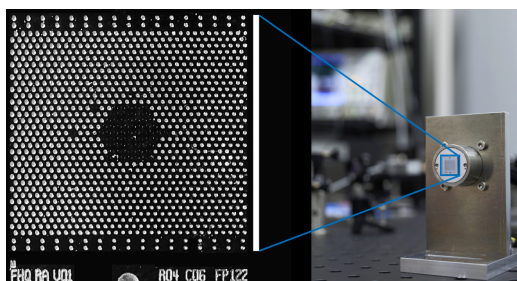


Figure 2. The integrated optical head assembly in a tiled-aperture configuration used in our OPA. There are 61 cleaved fiber emitters, separated by a pitch of  $250\mu\text{m}$ . An micro-lens array (not shown) is positioned at the output of the optical head to further increase fill-factor.

### 1.1.1 External vs. internal sensing

Control of the relative phase of individual emitters in an OPA can be achieved by measuring their optical phase at the output of the array. One way to do this involves interfering the light from each emitter with a reference local oscillator at a free-space photodetector. Another approach is to image the far field interference profile using a camera and a gradient descent algorithm. Optical phased arrays, such as these, that rely on free-space detection at the output of the array are referred to as *externally sensed*.

Phase can also be measured internally using the small amount of light back-reflected into each emitter at each fiber's glass-air interface. These so-called *internally sensed* OPAs have the advantage of not requiring external sensing optics, allowing them to be constructed entirely within optical fiber.<sup>4-6</sup> One disadvantage of internal sensing is, however, the introduction of what is called a  $\pi$ -phase ambiguity caused by light double-passing the same length of optical fiber. If the relative phase of two emitters at the output of the array is  $\pi$  radians, then upon passing through the same length of optical fiber twice it will appear to be  $2\pi$ . This means the two emitters appear to be in phase, when they are in fact 180 degrees out-of-phase at the output. The consequence of this is a potentially random distribution of optical power in the far field, degrading the OPA's performance. Since there can be no differentiation of the two scenarios by solely looking at the back-reflected signal, either extra precautions need to be taken or some form of external sensing needs to be used to check the output phase.

Externally sensed OPAs do not suffer from  $\pi$ -phase ambiguity since light passes through each length of optical fiber only once. The true phase of each emitter is thus measured directly at the output of the array. The OPA presented in this article uses external sensing to avoid the  $\pi$ -phase ambiguity associated with internal sensing.

## 2. SYSTEM ARCHITECTURE

Light from a narrow linewidth 1550 nm fiber laser is split into eight channels. Seven channels are guided through waveguide electro-optic modulators (EOMs) and connected to an optical head assembly (Fig. 3). The remaining channel is frequency shifted using an acousto-optic modulator to serve as a local oscillator for heterodyne detection.

Each emitter in the array is collimated using a micro-lenslet array, effectively increasing the OPAs fill-factor. Light exiting the array is interfered with the frequency shifted local oscillator using a free-space beam splitter and photodetector.

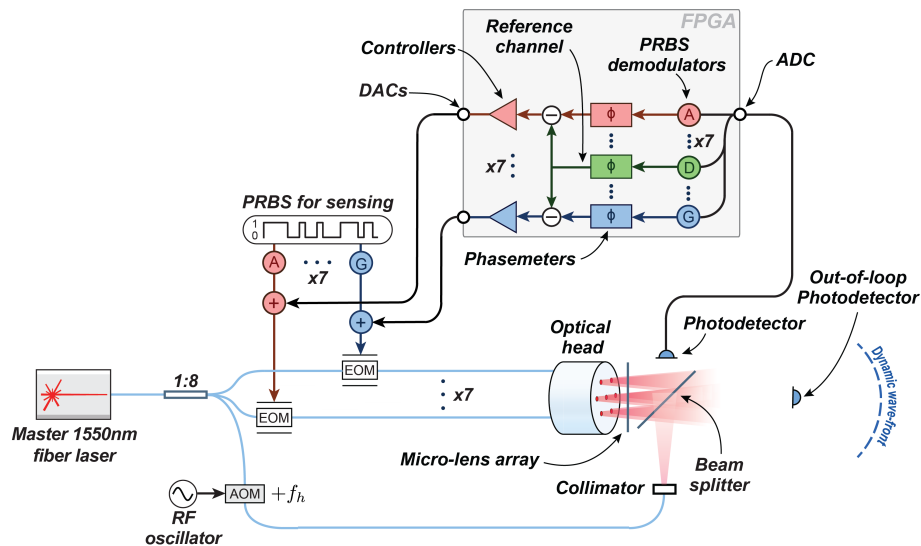


Figure 3. Experimental configuration of the optical and FPGA implemented digital signal processing systems required to offset phase lock the seven emitters.

The phase information of each channel is isolated in digital signal processing using Digitally Enhanced Heterodyne Interferometry which exploits spread-spectrum modulation techniques similar to those used in the Global

Positioning System.<sup>7</sup> The phase of each emitter is measured and controlled using separate phasemeters and controllers implemented on a field-programmable gate-array (FPGA). Feedback control signal is actuated via the electro-optic modulators.

## 2.1 Digitally Enhanced Heterodyne Interferometry

Digitally Enhanced Heterodyne Interferometry (DEHI) is a technique that allows the detection of multiple interferometric signals at a single photodetector without sacrificing the precision of conventional heterodyne interferometry.<sup>7</sup> DEHI works by exploiting the cross-correlation properties of pseudo-random bit sequences (PRBS) that are encoded onto the phase of the carrier field using an electro-optic modulator. The correlation properties of PRBS allow signals to be isolated based on their time-of-flight. One advantage of DEHI is that it reduces the complexity of the optical system, instead relying on the digital signal processing capabilities and scalability of FPGAs.

The specific class of PRBS encoded onto the phase of each channel is called a maximal-length sequence (m-sequence), which is produced by a linear feedback shift register that is efficiently implemented on an FPGA. The 10-bit m-sequence is encoded onto the phase of each channel at different delays and at a bit-rate of 12.5 MHz. The same pseudo-random code is applied to all emitter channels to exploit the good autocorrelation properties of m-sequences. Aboard the FPGA, multiple demodulators are run in parallel which apply different delayed versions of the m-sequence to the incoming data. This has the effect of demodulating only the heterodyne beat note signal with the same m-sequence delay. All other delays are seen as spread-spectrum noise which can be removed with digital filters.

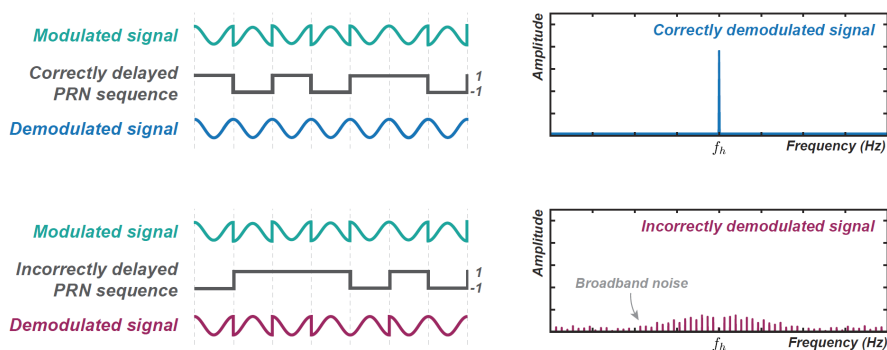


Figure 4. Time and frequency domain illustrations of correctly (top) and incorrectly (bottom) demodulated signals.<sup>6</sup>

## 2.2 Phasemeters

A phasemeter is an algorithm that tracks the phase of an oscillating signal. In our case, we use phasemeters to track the phase of the heterodyne beatnote for each channel in the OPA. There are many different possible architectures for phasemeters including zero-crossing detectors, IQ demodulation and phase-locked loops. For our particular application, we need a phasemeter that can offer very low latency throughput for high bandwidth feedback, has efficient implementation aboard the FPGA, and is able to track a tone with variable frequency. Zero crossing detectors are prone to false triggers in low signal-to-noise environments, and as such are ruled out for this application. IQ demodulation relies upon taking the arctangent operation of the in-phase and quadrature components, which is resource expensive to perform on an FPGA and suffers from increased latency. For these reasons, we have implemented a phase-locked loop phasemeter architecture since it can be efficiently implemented aboard the FPGA, offers high bandwidth, and can track tones of variable frequency.

A phase-locked loop architecture phasemeter generates a local oscillator tone whose phase is continuously updated to match that of the incoming tone. The relative phase error is detected by mixing the two tones together.

Let us begin with our input heterodyne beat note  $S_{input}(t)$  and local oscillator  $S_{LO}(t)$  which are both oscillating at a common frequency  $w$ :

$$S_{input}(t) = A \sin(\omega t + \phi_1) \quad (1)$$

$$S_{LO}(t) = B \cos(\omega t + \phi_2) \quad (2)$$

If we now mix  $S_{input}(t)$  and  $S_{LO}(t)$  we get:

$$S_{mixed}(t) = \frac{AB}{2}(\sin(\phi_1 - \phi_2) + \sin(2\omega t + \phi_1 + \phi_2)) \quad (3)$$

Applying a low-pass filter to attenuate the second harmonic at  $2\omega t$  and also applying the small angle approximation for sine ( $\sin(\theta) \approx \theta$  for  $\theta \ll 1$ ) yields:

$$S_{filtered}(t) = \frac{AB}{2} \sin(\phi_1 - \phi_2) \approx \frac{AB}{2}(\phi_1 - \phi_2) \quad (4)$$

Thus, if we continuously update the phase of our local oscillator such that the phase difference between it and the input signal is  $\theta \ll 1$ , then the error signal  $S_{filtered}(t)$  is linearly proportional to the phase difference between the beat note and local oscillator  $\phi_1 - \phi_2$ .

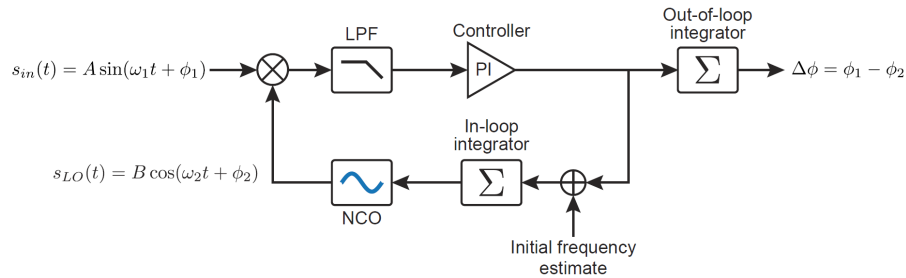


Figure 5. Schematic showing the architecture of the digitally implemented phase-locked loop.

The phasemeter (Fig. 5) is implemented aboard the FPGA, with the low-pass filter being a first-order cascaded-integrator comb design. The internal phase-locked loop controller is a proportional plus integral control architecture. The out-of-loop integrator is used to keep track of all corrections made to the numerically-controlled oscillator (NCO), and serves as the error source for the feedback control system for phase stabilization (see Sec. 2.3).

### 2.3 Feedback Control

The optical phase of each channel is actuated using electro-optical modulators (EOMs) (Fig. 3). The EOMs are responsible for applying both the pseudo-random noise codes and the path length stabilization signals for each channel. The controller architecture used to generate the feedback signals for the path length stabilization is also a proportional plus integral controller. The controller acts on the error signals generated by the out-of-loop integrator from the phasemeters running on each channel (Fig. 5). For beam steering, a phase offset can be applied at the out-of-loop integrator for each phasemeter. Since the controller will force the error to 0, the relative phase of each channel can be locked to any arbitrary point by applying this offset. Dynamic beam steering can be achieved by sweeping this phase offset so long as the sweep frequency is within the bandwidth of the feedback controller.

A phase wrapping algorithm is required at the output of the feedback controller since the EOMs have a limited actuation range of  $\sim 8$  cycles which can be extended by exploiting the  $2\pi$  ambiguity of phase. The threshold algorithm detects when the output signal passes either the upper or lower threshold, then wraps the output by an integer number of cycles. Padding values were added to prevent the rapid wraps of phase due to noisy signals when the output signal is close to a threshold. We chose a threshold value of  $\pm 0.6$  cycles with a padding of 0.2 cycles.

### 3. SYSTEM PERFORMANCE

The main metric of interest for the OPA is the relative phase error between emitters at the wavefront. A reduction in the relative phase noise will lead to a more coherent wavefront with better beam pointing precision. To measure this, we placed a second photodetector (labelled "Out-of-loop Photodetector" in Fig. 3) at the second port of the beam-splitter in the far field and ran the OPA in a 2-emitter configuration. To make a true out-of-loop phase measurement, we connected the second out-of-loop photodetector to two separate phasemeters with pseudo-random code demodulators at the two delays corresponding to each emitter. The phase in the out-of-loop integrators in the phasemeters were then simultaneously recorded, with their difference being taken in post processing. It should be noted that whilst the phasemeters were implemented aboard the same FPGA as the in-loop phasemeters used for path length stabilization, they were in no way linked to ensure a true out-of-loop measurement. The results of this differential wavefront phase measurement can be seen in Fig. 6. The free running (purple) trace shows the differential phase drifting due to thermal and acoustic noise in the fibers, whilst the stabilized (green) trace shows greatly reduced phase error. The differential RMS phase error was measured to be  $25.6\text{mRad}$ , or  $\theta_{RMS} = \lambda/245$  cycles, where  $\lambda$  is the wavelength of the 1550 nm carrier.

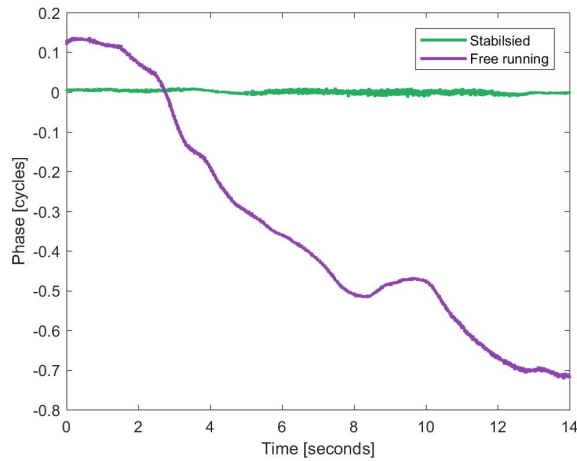


Figure 6. Time series measurement of the out-of-loop differential wavefront phase ( $\phi_{ch1} - \phi_{ch2}$ ) with path length stabilization on (green) and free running (purple).

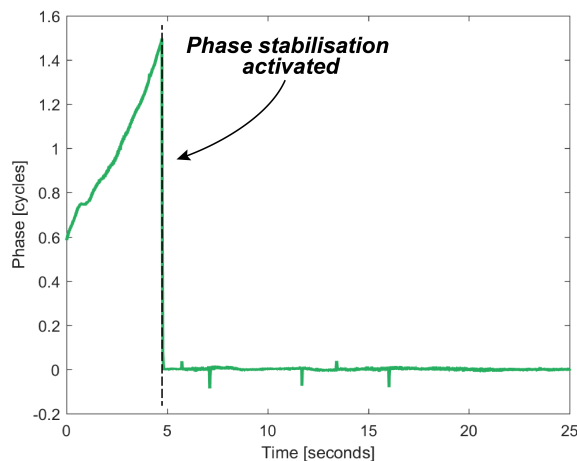


Figure 7. Time series measurement of the out-of-loop differential wavefront phase with phase locking activated at 4.8 seconds.

A time-series plot showing phase stabilization being activated can be seen in Fig. 7. The small peaks visible



once the controller is activated are caused by slight errors in the phase-wrapping voltage used to extend the actuation range of the EOMs. These slight voltage errors cause the phase to wrap by slightly more or less than  $2\pi$ , resulting in a low-magnitude phase step that is measured by the phasemeter every time a phase-wrap transition occurs. These features can be removed entirely by calibrating the voltage applied to each EOM.

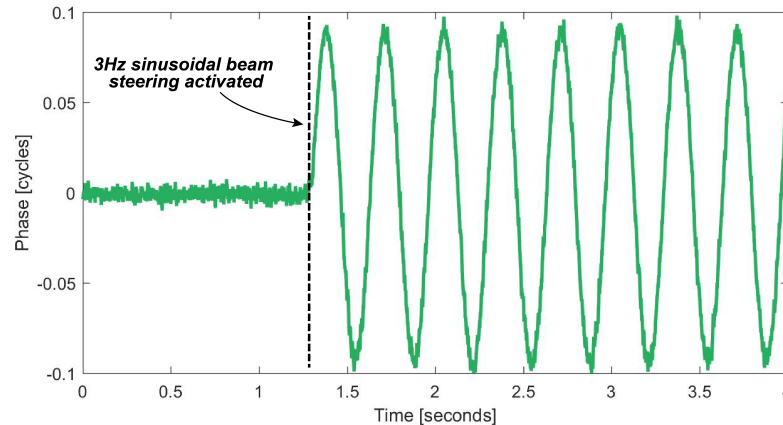


Figure 8. Time series measurement of a 3Hz sinusoidal steering signal with an amplitude of 0.1 cycles.

Dynamic beam steering was demonstrated experimentally by injecting a 3 Hz sinusoidal offset with an amplitude of 0.1 cycles to the phase measurement for channel 1 (Fig. 8). This is equivalent to injecting a signal into the error point of the control loop where the control system then imposes this signal onto the output. Whilst this demonstration only uses two emitters, it is simple to scale this to more emitters as the project advances.

#### 4. CONCLUSIONS AND FUTURE WORK

We have presented the preliminary results of a 7-emitter 1550 nm OPA for solid state beam pointing. Our OPA uses DEHI implemented on an FPGA to measure the phase of each emitter in the OPA and is able to feedback via EOMs to stabilize the optical path lengths of each channel against vibrations and thermal changes, maintaining the relative phase of each of the emitters. Our system is able to achieve an RMS phase stability between emitters of  $\lambda/245$  cycles, which is sufficient to enable sub-milliradian pointing precision. By changing the error point of the control loop, we are able to arbitrarily control the phase of an individual emitter, providing us with control of the interference pattern in the far field and thus the ability to ‘steer’ the beam.

More careful calibration of the voltage required to be applied to the EOMs to change the phase of the 1550 nm carrier by  $2\pi$  radians will mitigate the small phase steps seen when phase-wrapping occurs. The steering bandwidth of the OPA is currently limited to a few kHz by the electronics used to combine both the 12.5 MHz PRBS and low frequency feedback signals onto each EOM. Higher bandwidth commercial units, or units built in house, will enable a steering bandwidth of a few MHz, allowing the OPA to very rapidly interrogate a field of regard or ‘snap back’ during a scanning sequence. With improved modelling and understanding of the digital control system, we will be better able to optimize the gains of the phasemeter and feedback controllers, allowing us to reduce the RMS phase error still further and achieve micro-radian pointing precision, which is needed for long range free space laser links such as for satellite communications.

#### ACKNOWLEDGMENTS

This work was partially funded by the Australian Research Council Centre of Excellence for Gravitational Wave Discovery (OzGrav) (project ID CE170100004) and the Australian Research Council Centre of Excellence for Engineered Quantum Systems (EQUS) (project ID CE170100009).



## REFERENCES

- [1] B. S. Robinson, D. M. Boroson, D. A. B. D. V. M., “Overview of the lunar laser communications demonstration,” *Proc.SPIE* **7923**, 7923 – 7923 – 4 (2011).
- [2] Wuchenich, D. M. R., Mahrtdt, C., Sheard, B. S., Francis, S. P., Spero, R. E., Miller, J., Mow-Lowry, C. M., Ward, R. L., Klipstein, W. M., Heinzl, G., Danzmann, K., McClelland, D. E., and Shaddock, D. A., “Laser link acquisition demonstration for the grace follow-on mission,” *Opt. Express* **22**, 11351–11366 (May 2014).
- [3] Hecht, J., “Lidar for self-driving cars,” *Optics and Photonics News* **29**(1), 26–33 (2018).
- [4] Roberts, L. E., Ward, R. L., Francis, S. P., Sibley, P. G., Fleddermann, R., Sutton, A. J., Smith, C., McClelland, D. E., and Shaddock, D. A., “High power compatible internally sensed optical phased array,” *Optics express* **24**(12), 13467–13479 (2016).
- [5] Roberts, L. E., Ward, R. L., Sutton, A. J., Fleddermann, R., de Vine, G., Malikides, E. A., Wuchenich, D. M., McClelland, D. E., and Shaddock, D. A., “Coherent beam combining using a 2d internally sensed optical phased array,” *Applied optics* **53**(22), 4881–4885 (2014).
- [6] Roberts, L. E., *Internally Sensed Optical Phased Arrays*, PhD thesis, Research School of Physics and Engineering, The Australian National University (2016).
- [7] Shaddock, D. A., “Digitally enhanced heterodyne interferometry,” *Optics letters* **32**(22), 3355–3357 (2007).